



HEDLA 2022

Flash Poster Presentation

#03 D. Russell <i>Radiatively cooled shocks in jets at the MAGPIE pulsed-power facility</i>	#04 K. Sakai <i>Local measurements of laser-driven electron-scale magnetic reconnection</i>	#08 V. Tranchant <i>New Class of Laboratory Astrophysics Experiments: Application to Radiative Accretion Processes Around Neutron Stars</i>	#09 F. Cruz <i>Particle-in-cell simulations of laser-driven, ion-scale magnetospheres in laboratory plasmas</i>	#10 H. Hasson <i>Experimental results from a pulsed-power platform to study accretion-driven astrophysical outflows</i>
#12 E. Figueiredo <i>Kinetic models in neutron star charge starved vacuum gaps</i>	#13 S. Antunes <i>Time resolved opacity maps of warm dense Ti: a Bayesian search of coupling parameters</i>	#18 R. Babjak <i>Direct laser acceleration enhancement using plasma density modulations</i>	#19 B. Martinez <i>Ultra-high-intensity lasers for channel acceleration of positrons</i>	#21 W. Zhang <i>Strong-field QED features in the leptonic beam collision</i>
	#22 O. Amaro <i>Electron beam and photon distribution functions after a laser-electron scattering: analytical model accounting for 3D focusing geometry and non-ideal spatio-temporal synchronization</i>	#25 P. Bilbao <i>Synchrotron cooling as a progenitor of kinetic instabilities and coherent radiation</i>	#31 D. Maslarova <i>Transient Relativistic Plasma Grating to Tailor High-Power Laser Fields, Wakefield Plasma Waves, and Electron Injection</i>	

Radiatively cooled shocks in jets at the MAGPIE pulsed-power facility

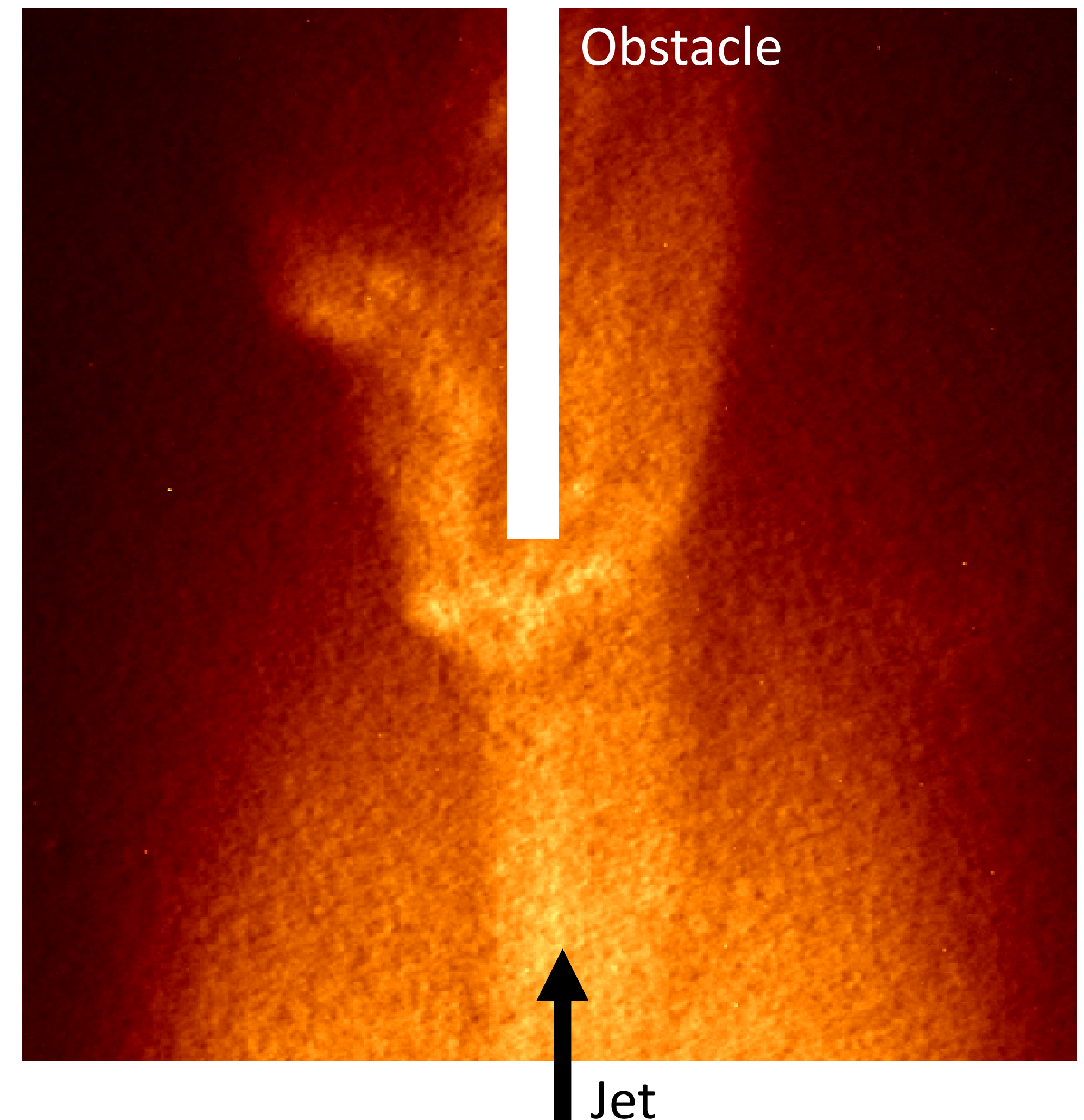
Pulsed power driven foil produces a supersonic jet

The jet collides with a small obstacle

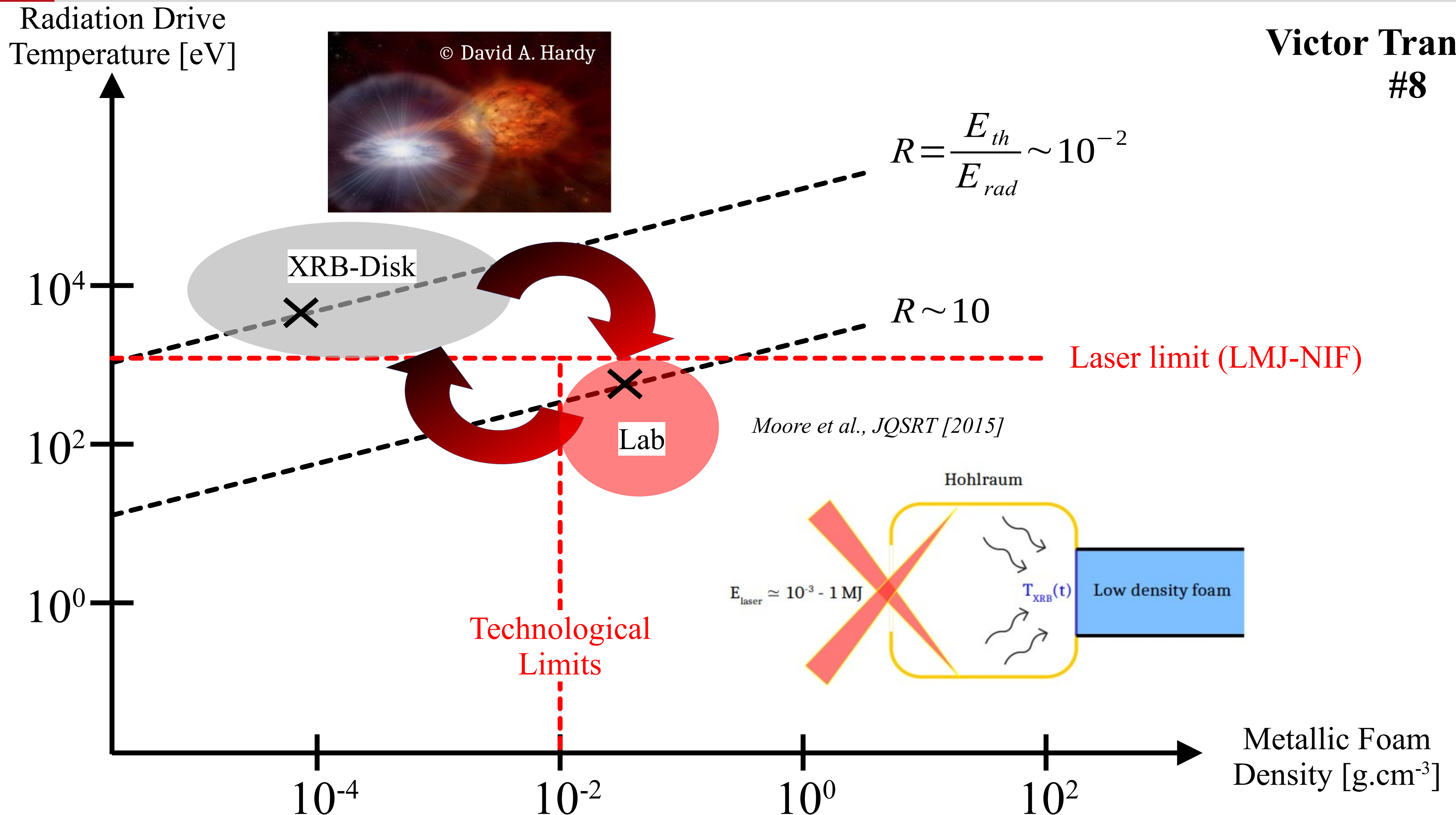
The resulting shock is clumpy

We believe this is caused by radiative cooling instabilities

These experiments are relevant for understanding the complex structures seen in protostellar jets



**Victor Tranchant
#8**

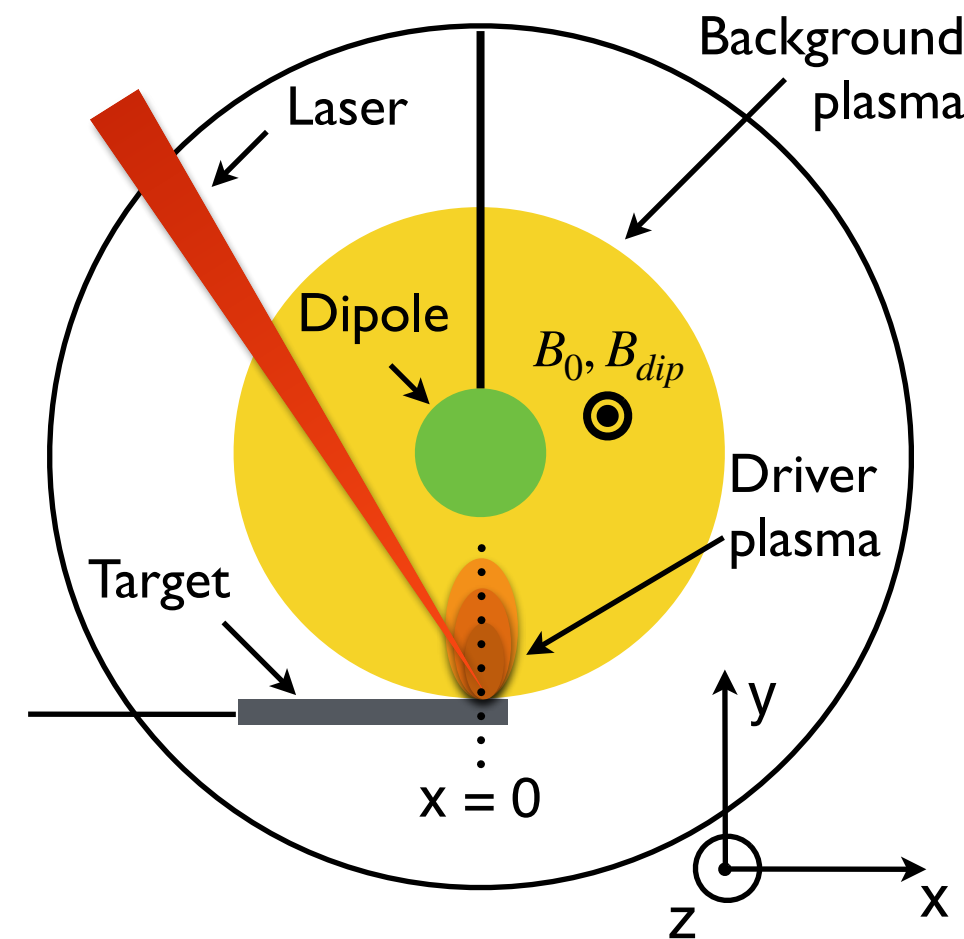


Particle-in-cell simulations of laser-driven, ion-scale magnetospheres in laboratory plasmas (#09)

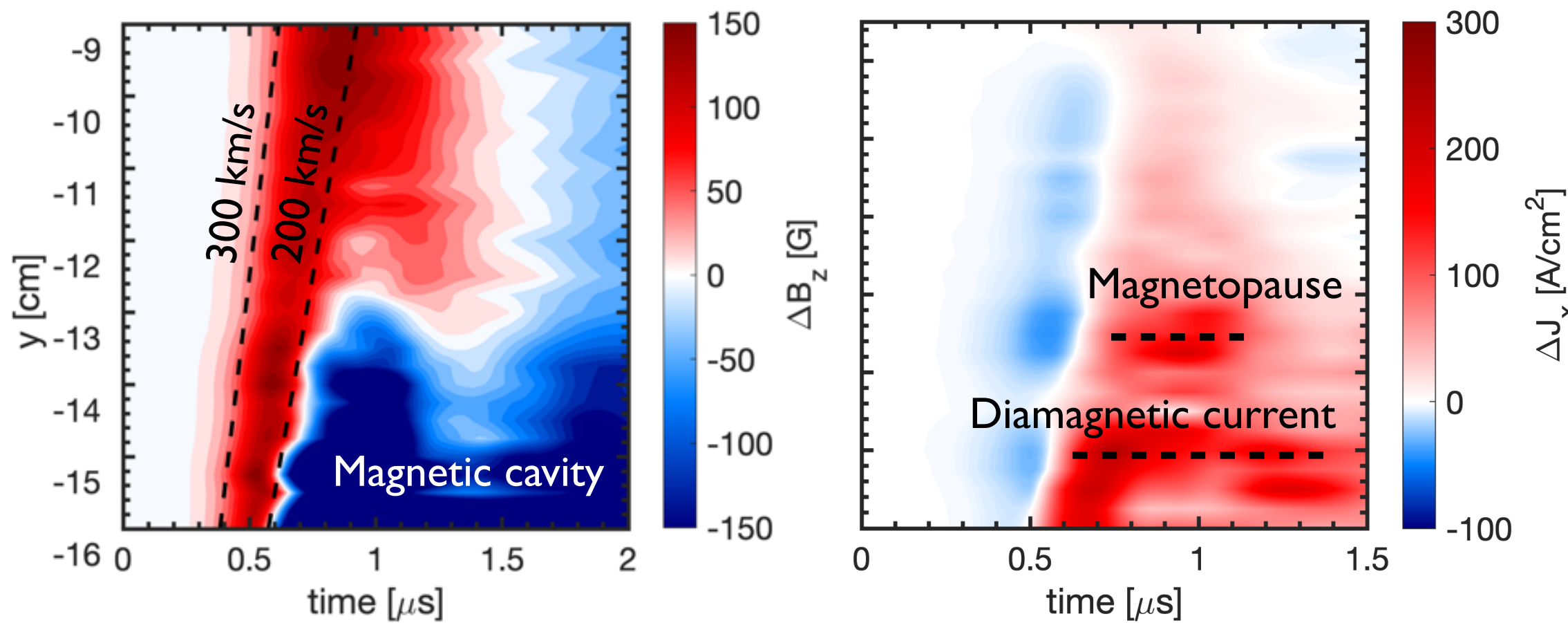
Mini-magnetospheres in laboratory*

In the Large Plasma Device (LAPD), a laser was focused into a plastic target, releasing a driver against a magnetized background plasma.

By inserting a current loop, a mini magnetosphere was created in the laboratory.



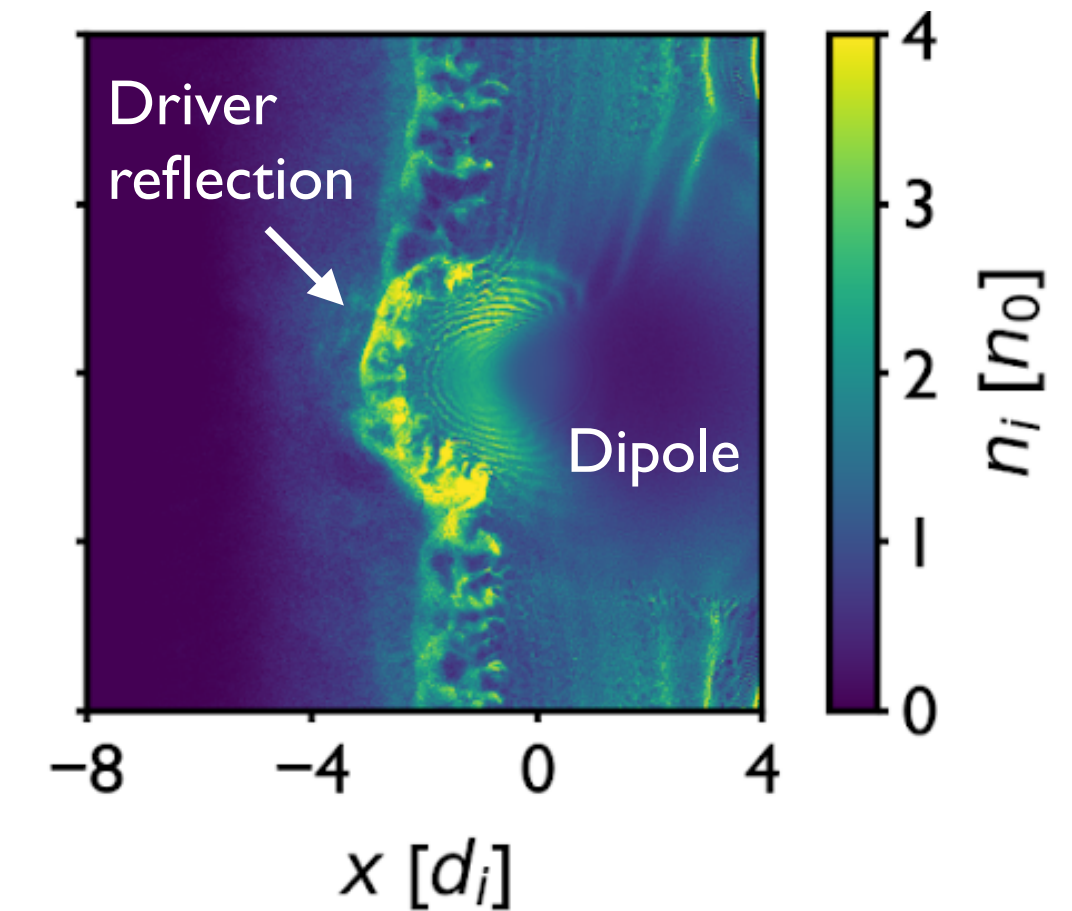
Magnetic field streak plot at $x = 0$: Current density streak plot at $x = 0$:



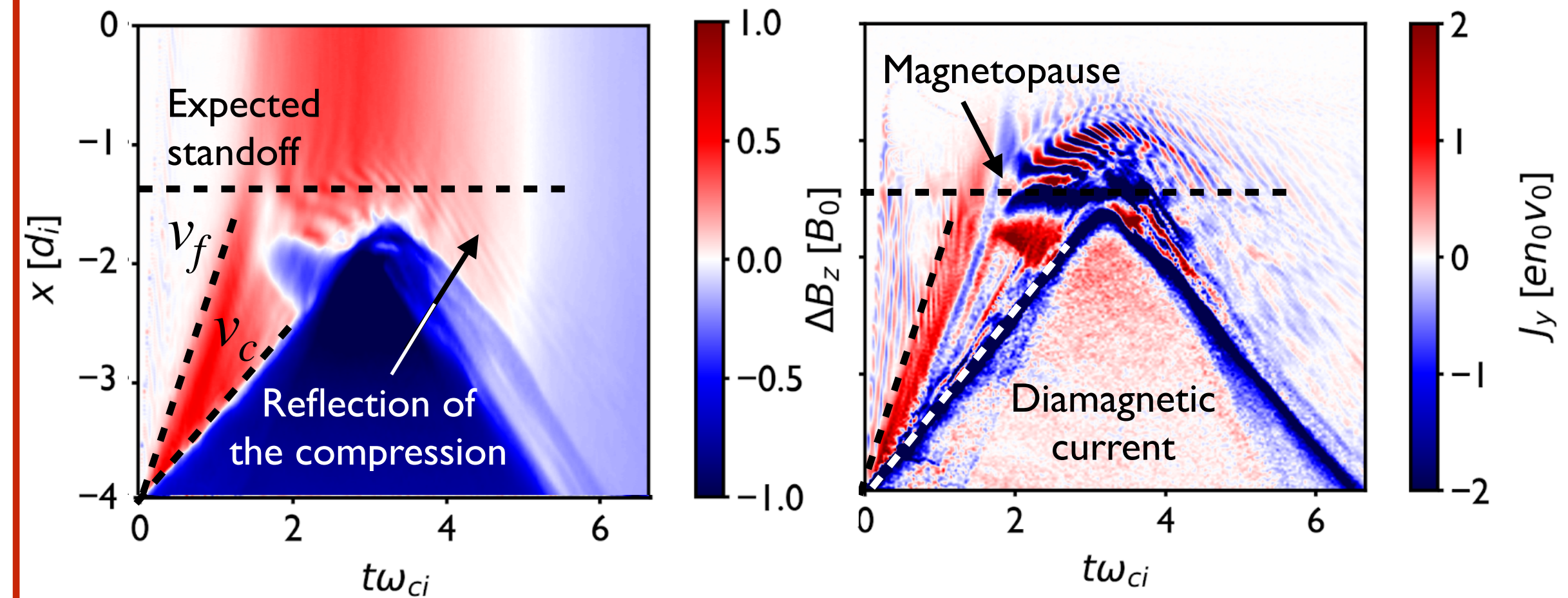
Overall dynamics of PIC simulations**

To validate the experimental results, 2D particle-in-cell (PIC) simulations were performed with OSIRIS.

Multiple parameters scans showed the importance of each system parameter in the magnetospheric structures observed.



The simulation results are consistent with the LAPD experiments:





Experimental results from a pulsed-power platform to study accretion-driven astrophysical outflows



H. Hasson et al., U. of Rochester

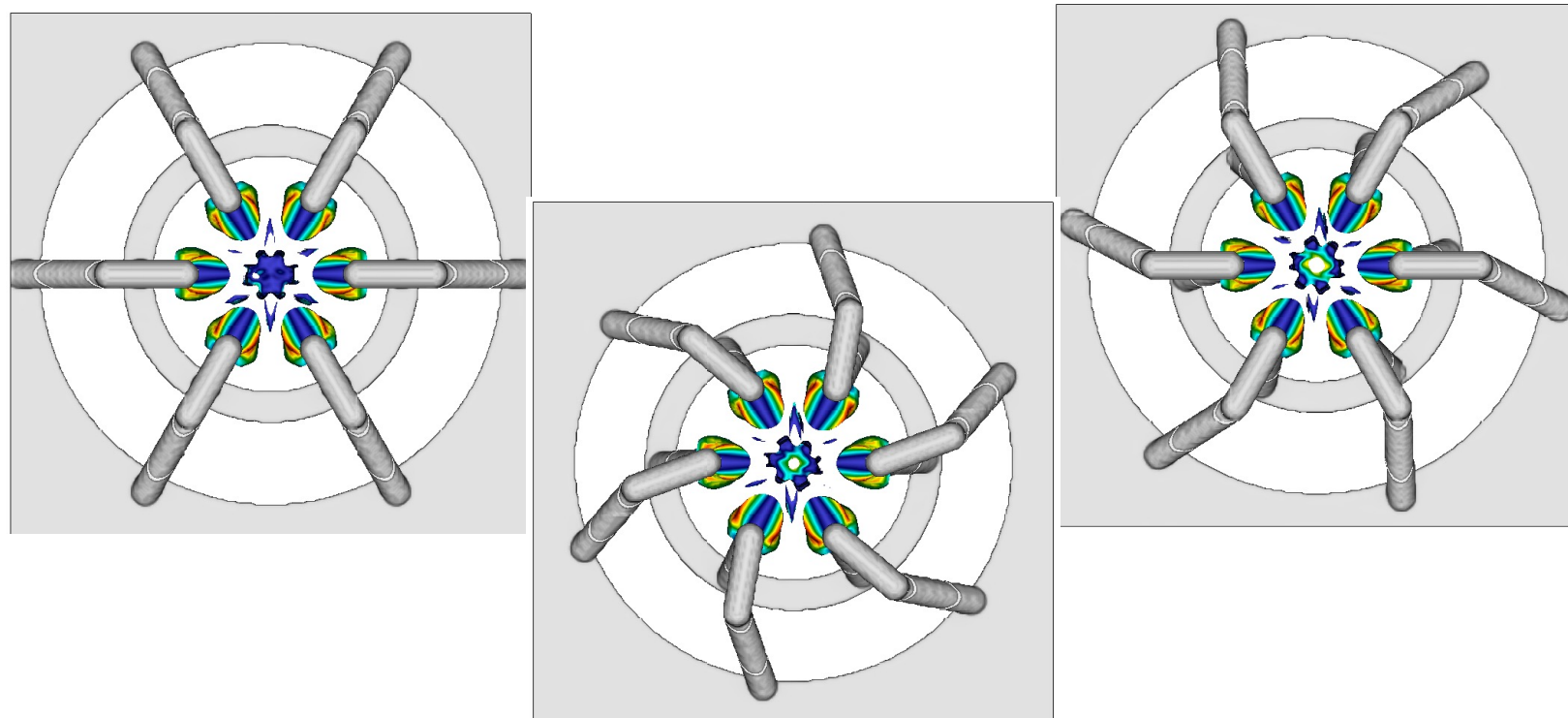
Poster #10

Load design

modified cylindrical wire array

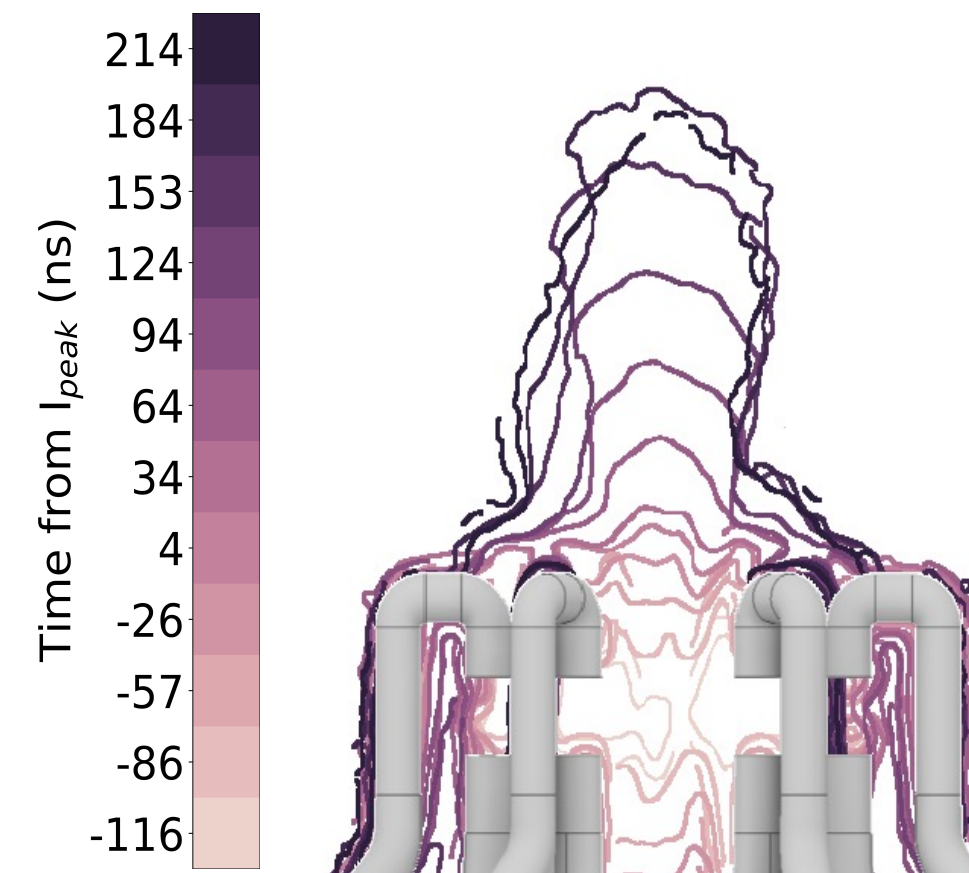


Independently control rotation and B_z to influence disk -> jet transition

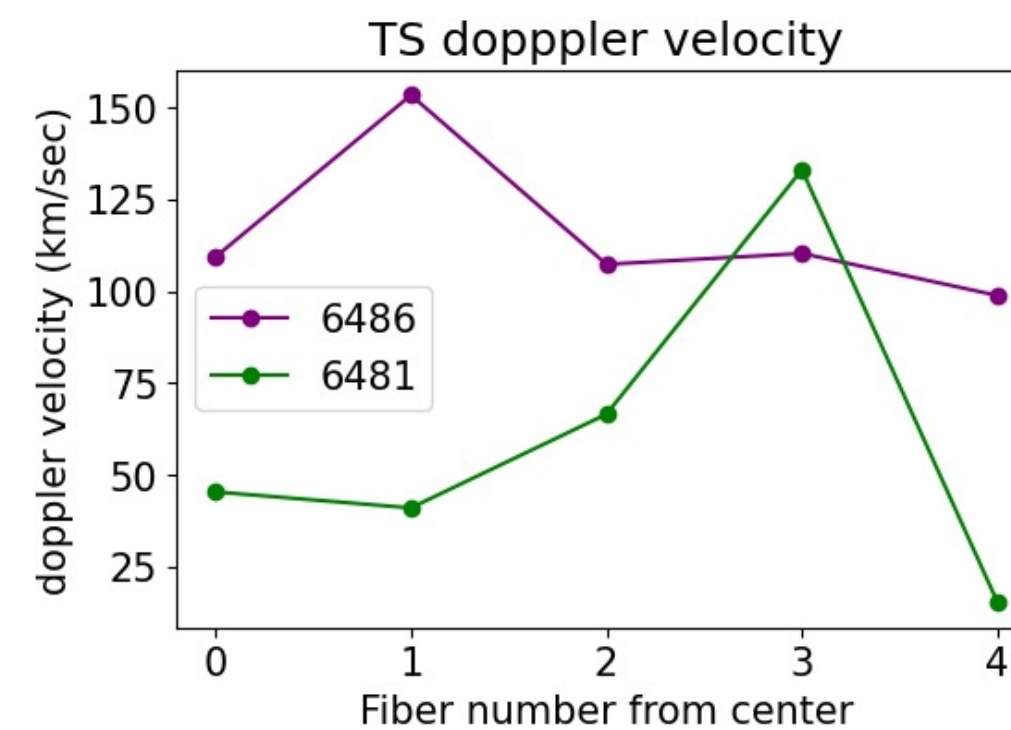


Velocity measurements

Vertical front tracing: ~ 100 km/s

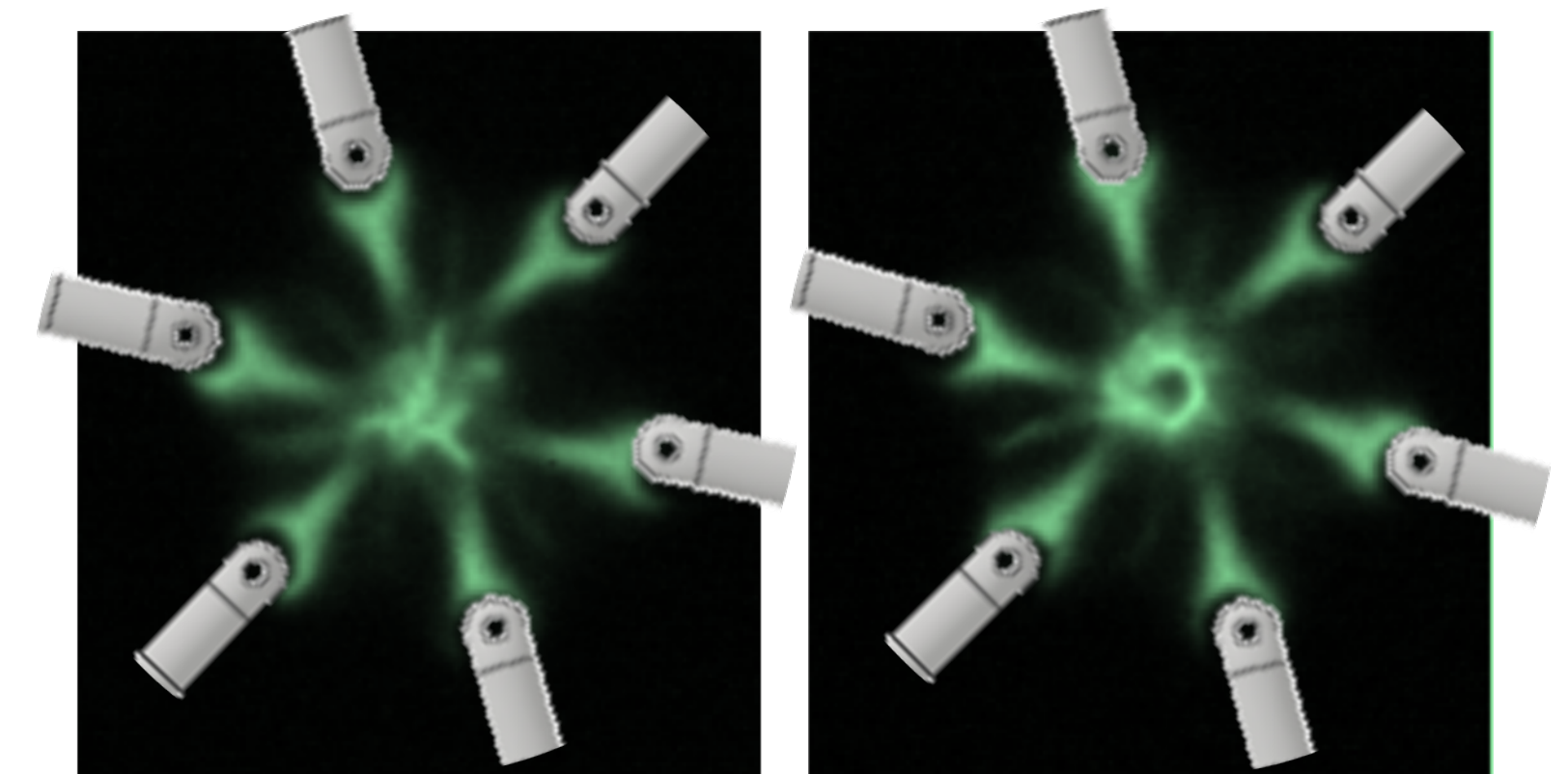


Radial Thomson scattering fits: ~ 100 km/s

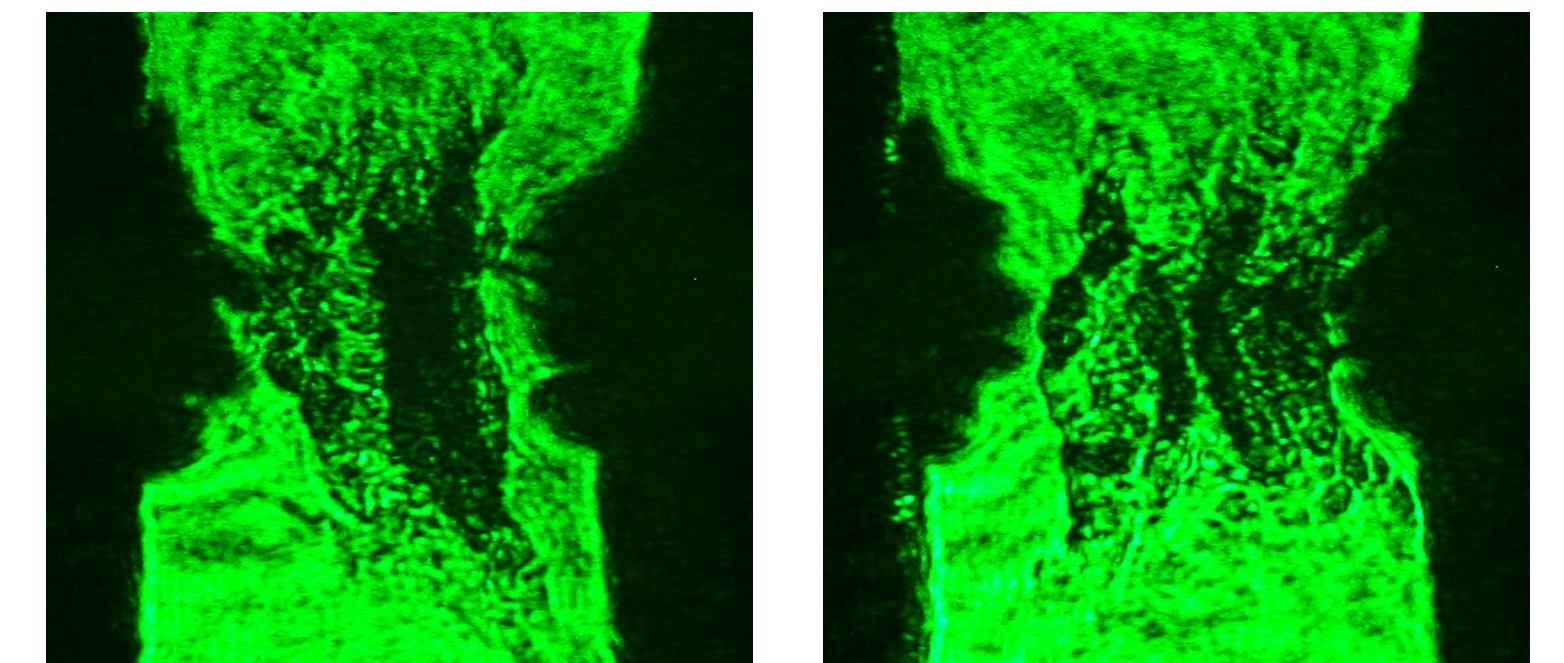


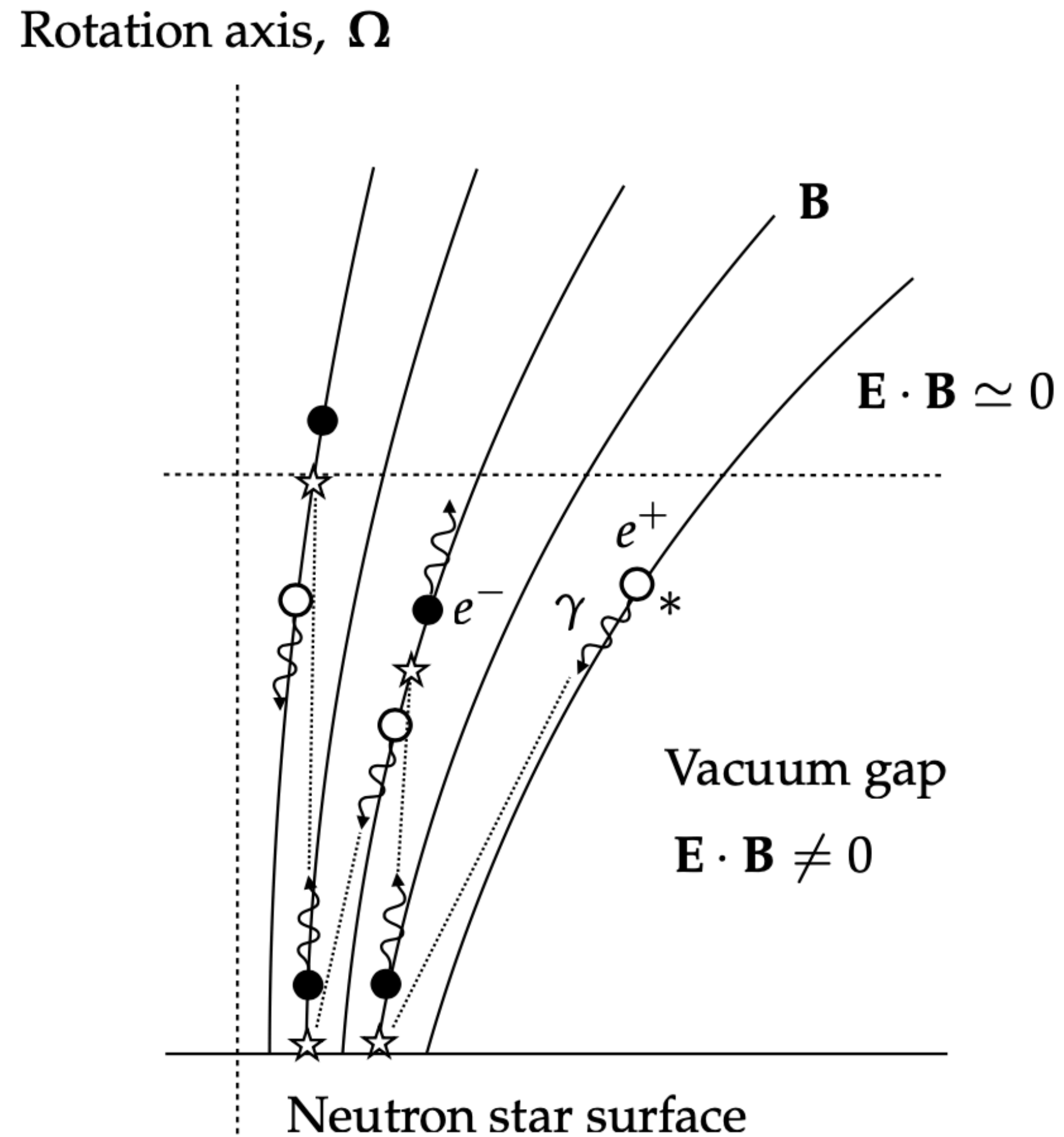
Imaging

XUV Above view: Filled vs hollow (rotating) outflows



Side-on shadowgraph: Filled vs hollow (rotating) outflows





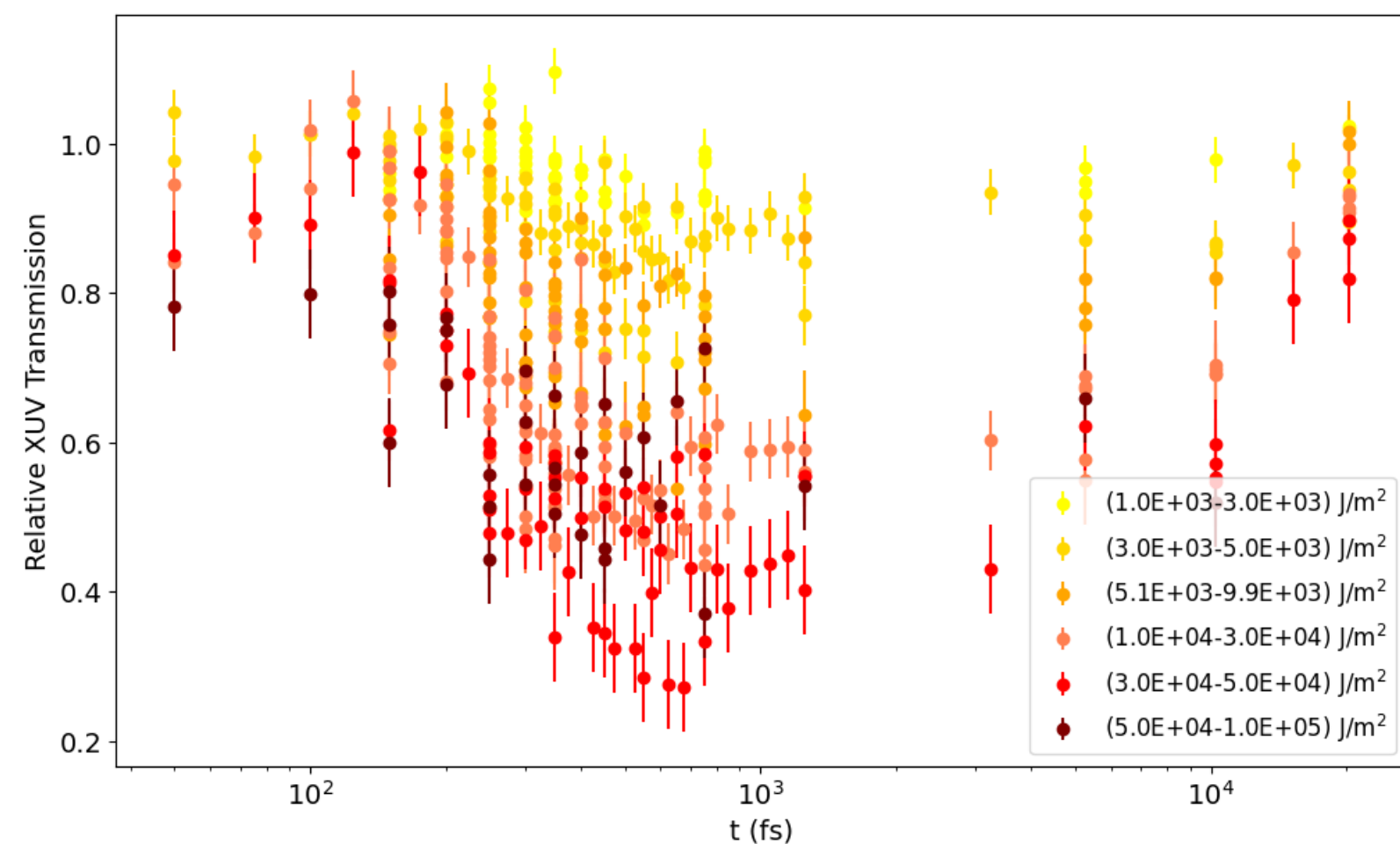
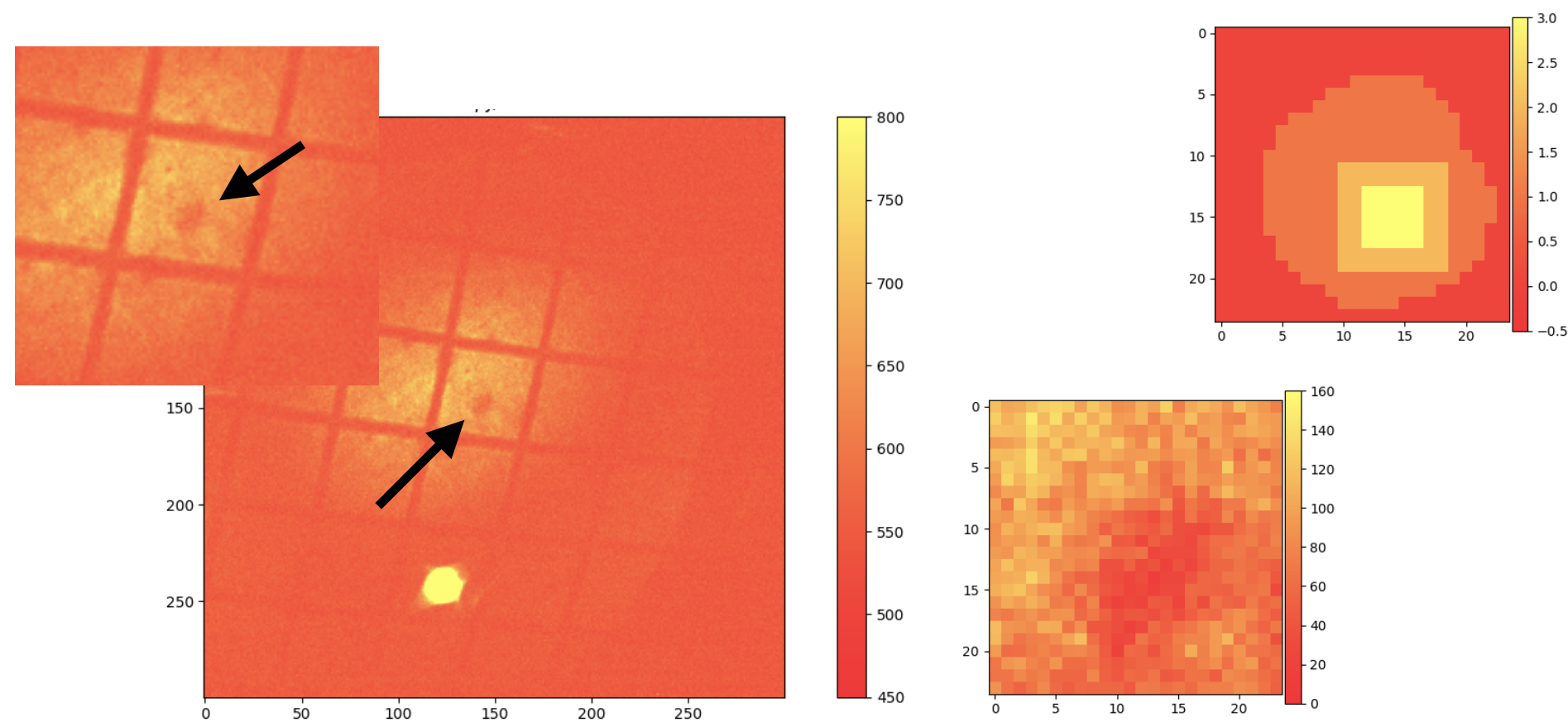
- Exponential production of $e^+ - e^-$ plasma
- Analytical model of the cascade behaviour from first principles
- Allows extension to other astrophysical scenarios and laboratory experiments

Time Resolved Studies of Warm Dense Titanium

The ill defined nature of measurements in Warm Dense States and the many uncertainties favours a statistical approach, for which big data sets are needed.

Results

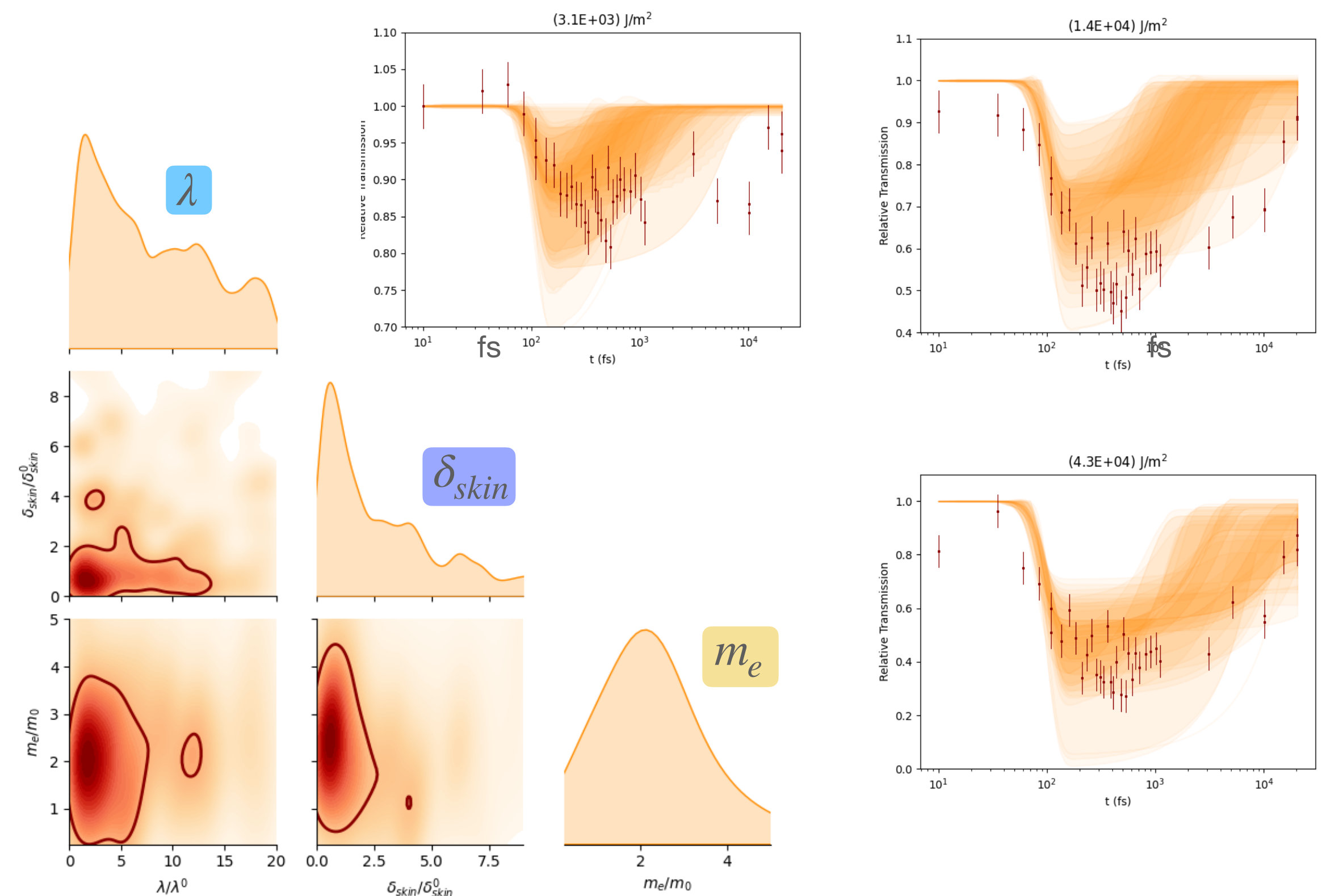
Isochorically heated warm dense Titanium, probed near the $M_{2,3}$ absorption edge.



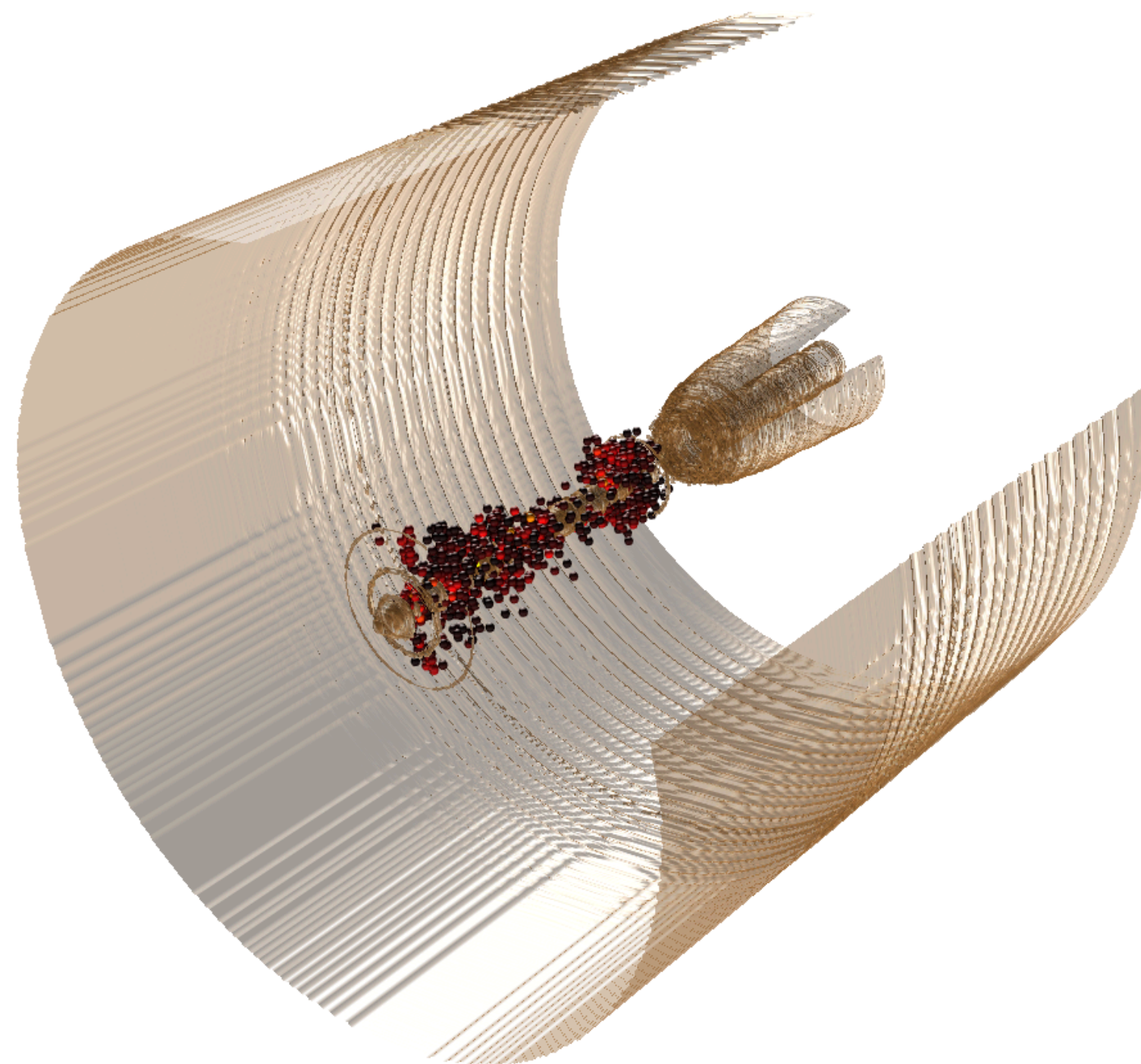
Two Temperature Model

$$\int_{-\infty}^{+\infty} \frac{\partial f(\epsilon, \mu, T_e)}{\partial T_e} g(\epsilon) \epsilon d\epsilon \cdot \frac{\partial T_e}{\partial t} = S(r, t) - \frac{\pi \hbar k_B \lambda \langle \omega^2 \rangle}{g(\epsilon_F)} \int_{-\infty}^{+\infty} g^2(\epsilon) \left(-\frac{\partial f}{\partial \epsilon} \right) d\epsilon \cdot (T_e - T_l) G_{e-i}$$

$C_e(T_e)$



Electrons can be accelerated by the Direct Laser Acceleration only up to the maximum energy γ_{max} defined by the plasma density and the integral of motion



Conserved quantities

Constant density



$$I = \gamma - \frac{p_x}{m_e c} + \frac{y^2 \omega_p^2}{4c^2}$$

Varying density

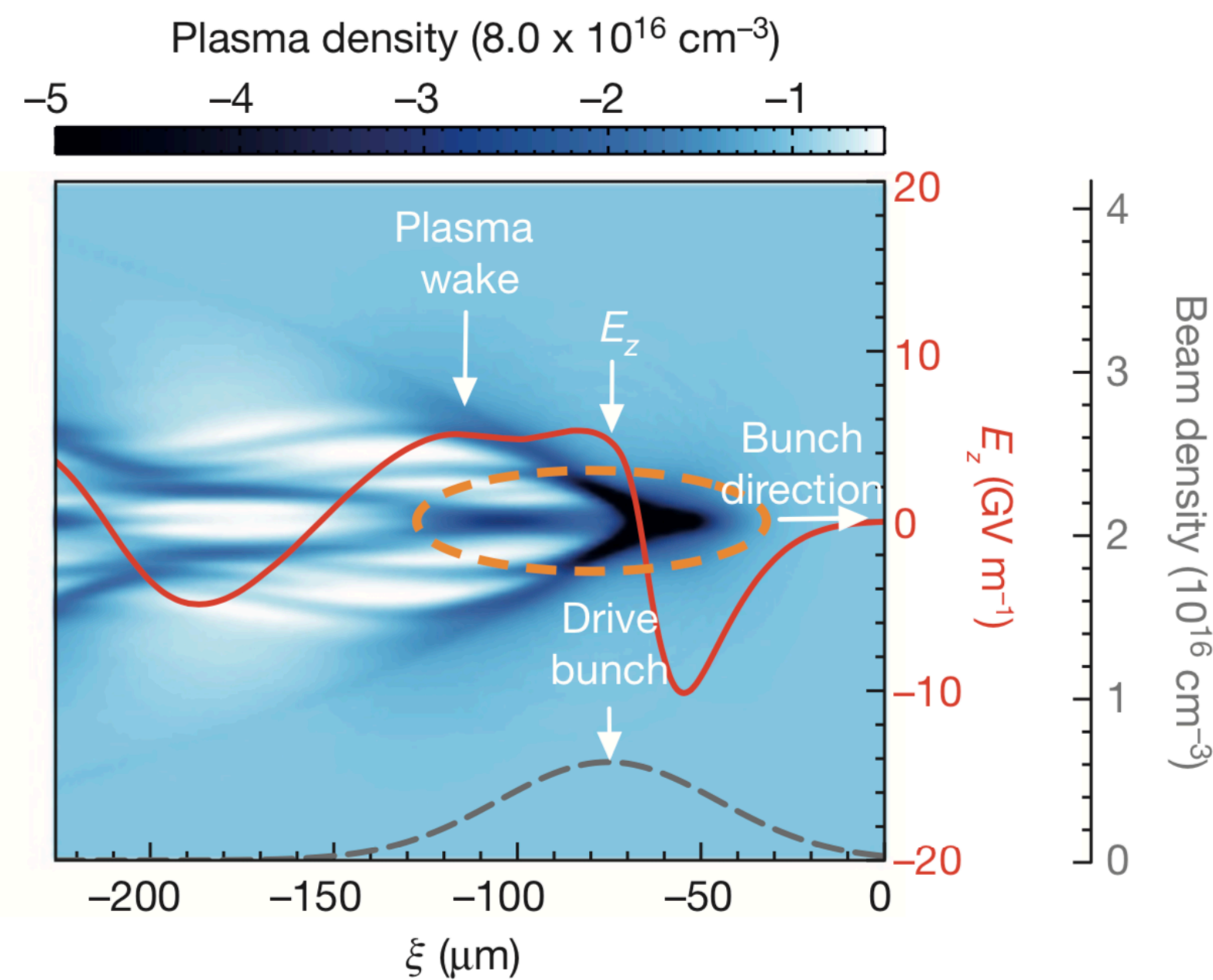


$$\gamma_{max} = 2I^2 \left(\frac{\omega_0}{\omega_p} \right)^2$$



At plasmas with density gradient the maximum achievable energy of electrons is defined by the initial conditions at the moment of resonance

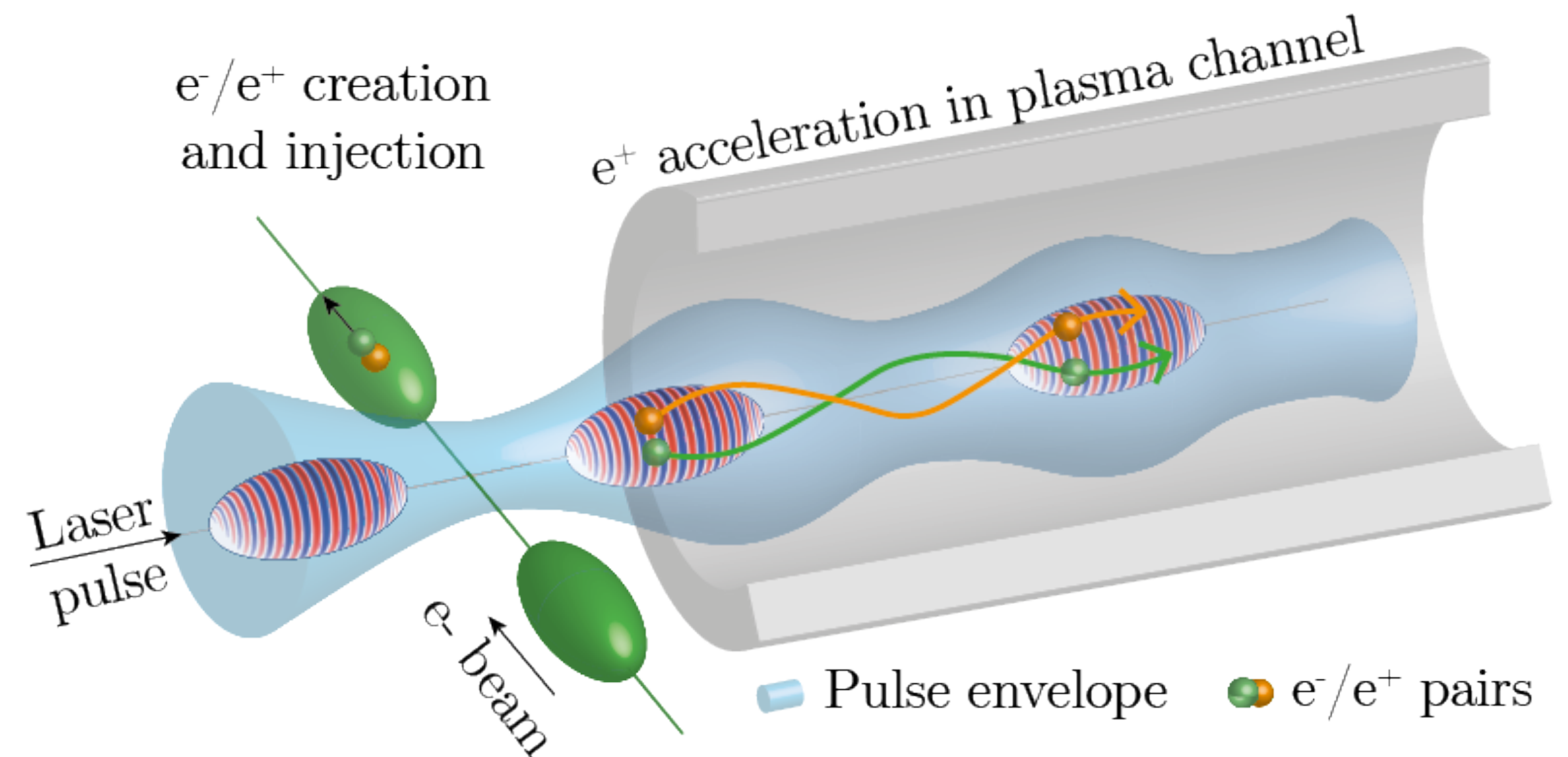
Wakefield acceleration¹



Positrons are created
by an accelerator

¹S. Corde et al, Nature, 524 442-445 (2015)

Multi-PetaWatt laser²



Positrons are created
by the pulse

²B. Martinez et al, to be submitted

Background and motivation

- ◆ Leptonic (electron-positron) beam collision provides a platform where various fundamental physics can be studied.
- ◆ Beam collision in the mild QED regime ($\chi_e \lesssim 1$) has been studied [2], but the study on the strong QED regime ($\chi_e \gg 1$) is still in its infancy [3].

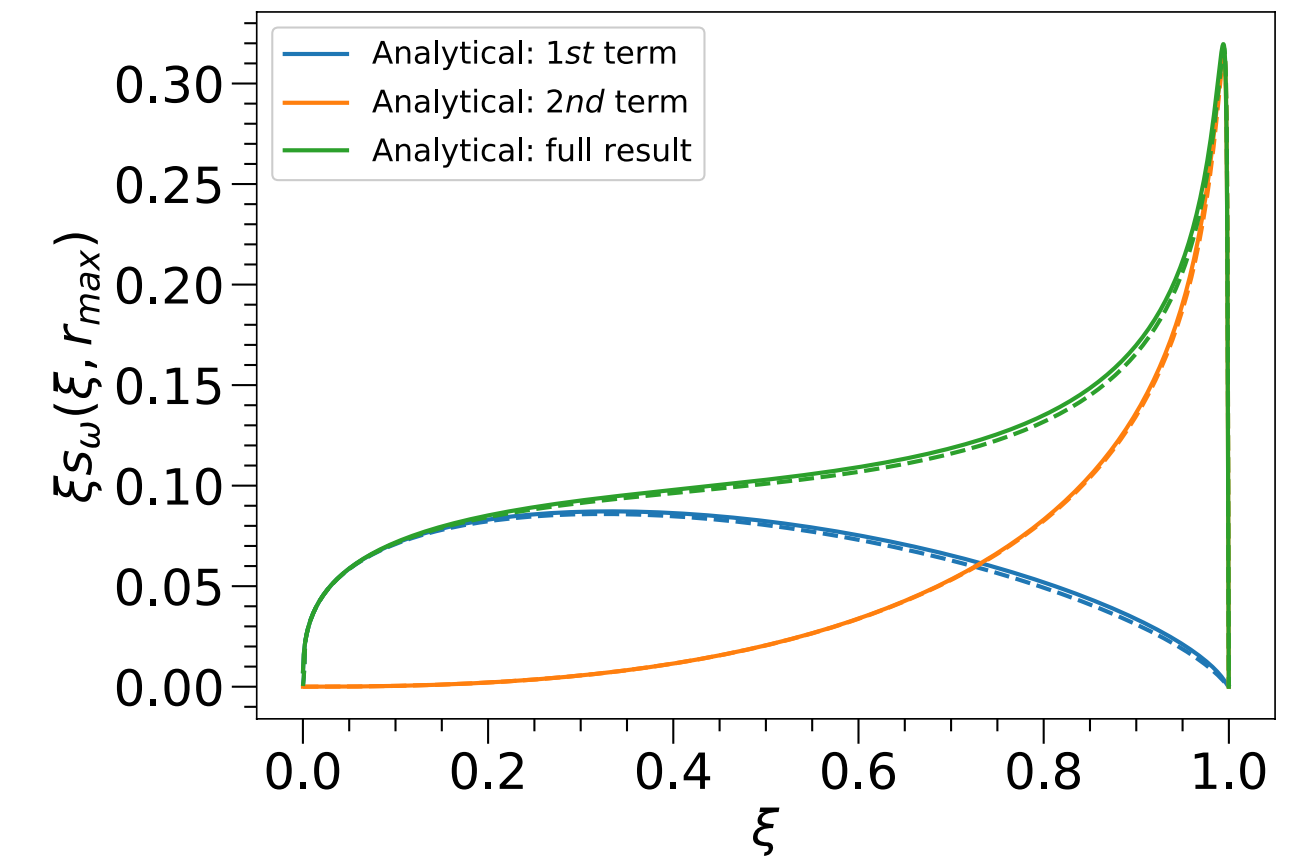
$$\chi_e = \frac{1}{E_s} \sqrt{\left(\gamma \vec{E} + \frac{\vec{p} \times \vec{B}}{mc}\right)^2 - \left(\frac{\vec{p} \cdot \vec{E}}{mc}\right)^2} \simeq \frac{2\gamma E_\perp}{E_s}$$

$$W_\omega = \frac{\alpha}{\sqrt{3}\pi\tau_c\gamma} \left[\int_b^\infty dq K_{5/3}(q) + \frac{\xi^2}{1-\xi} K_{2/3}(b) \right]$$

$$b = \frac{2}{3\chi_e} \frac{\xi}{1-\xi}$$

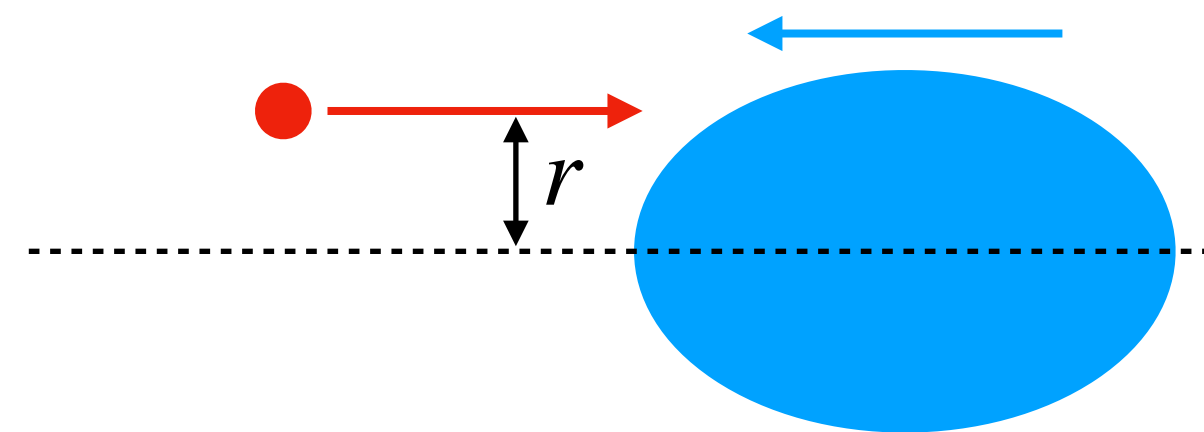
Applications: Theory & Dedicated collision config.

- ◆ Excellent agreement with theory
- ◆ Sharp peak is present at $\xi \rightarrow 1$



Photon spectrum $s_\omega(\xi, r)$ emitted by a single particle

$$s_\omega(\xi, r) = \int_{-\infty}^{\infty} W_\omega dt$$

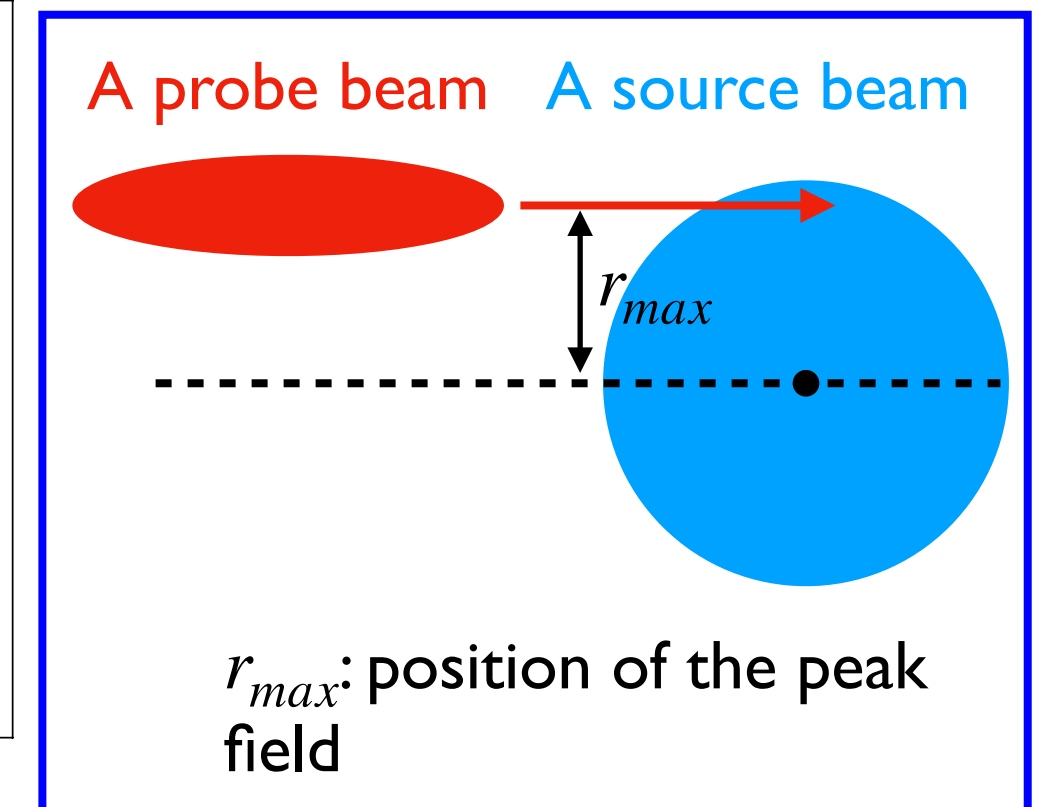
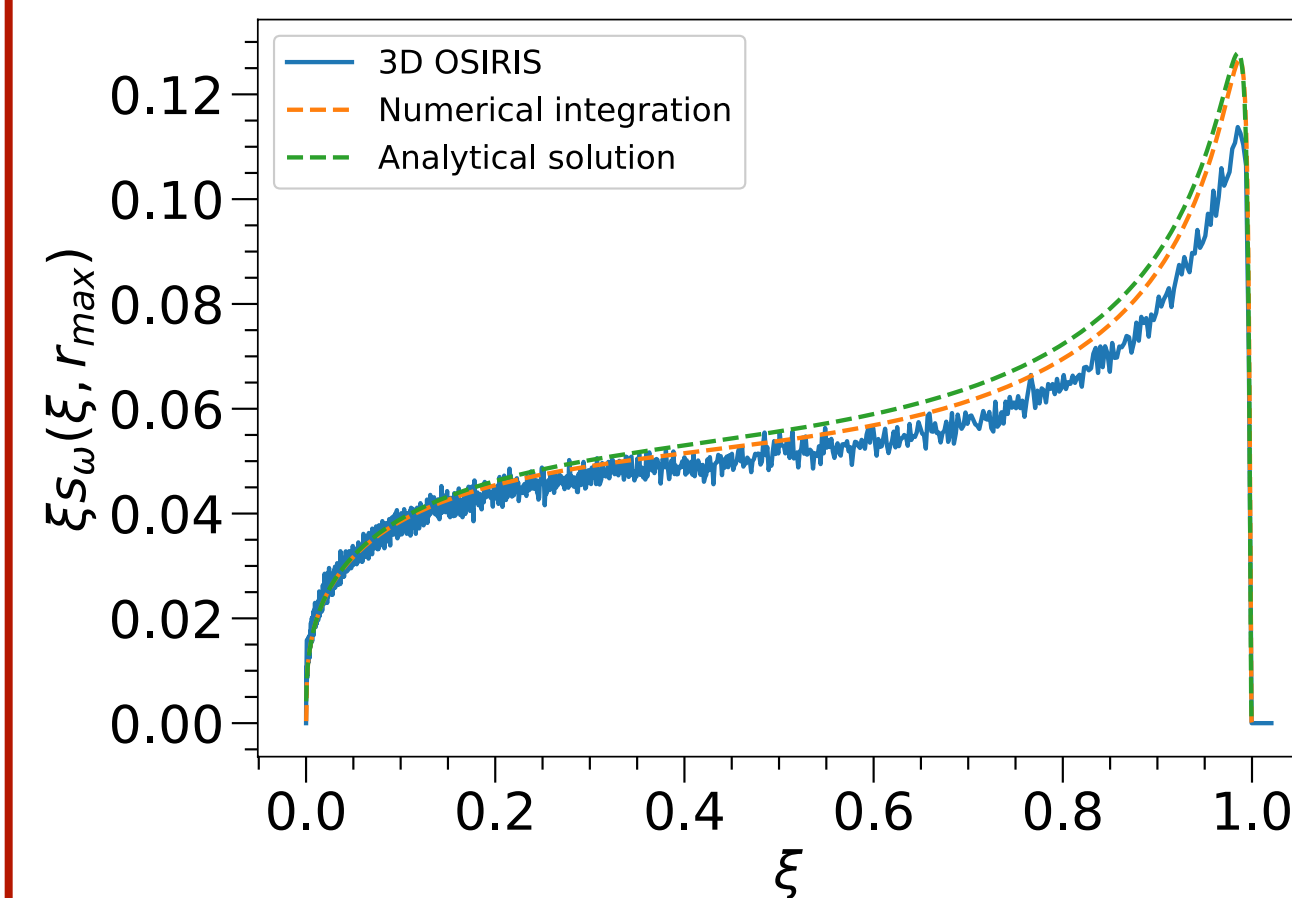


$$s_\omega(\xi, r) = \frac{\alpha\sigma_z}{\sqrt{6}\pi\tau_c\gamma c} \left(k_{5/3} + k_{2/3} \frac{\xi^2}{1-\xi} \right) C_b^{-2/3} \exp(-C_b) \cdot U \left[\frac{1}{2}, \frac{5}{6}, C_b + p_0 \right]$$

* Fitting constant: $k_{2/3} = 1.23$ and $k_{5/3} = 2k_{2/3}$

$$C_b = \frac{2}{3\chi_{emax}} \frac{\xi}{1-\xi} \frac{F(r_{max})}{F(r)}$$

A dedicated collision configuration



[1] W. L. Zhang, T. Grismayer, L. O. Silva, *in preparation*, 2022.

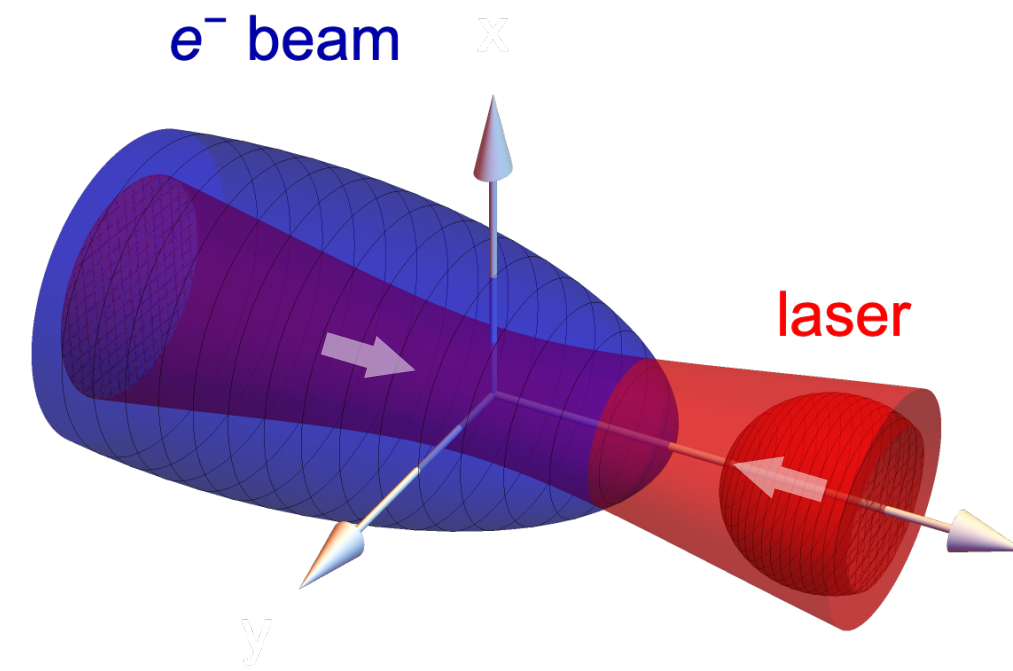
[2] F. Del Gaudio, et al., PRAB, **22**, 023402 (2019). [3] Matteo Tamburini, Sebastian Meuren, arXiv:1912.07508v2 (2020).

Motivation

Nonlinear Compton Scattering (γ -ray emission) and Breit-Wheeler e^+e^- pair production will be common in near future laser facilities.

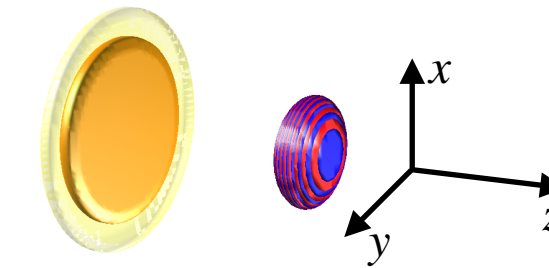
Standard numerical modelling of these experiments is accomplished using heavy 3D PIC-QED simulations.

We develop a semi-analytical model for the final photon and electron spectra to accelerate experiment design and interpretation.



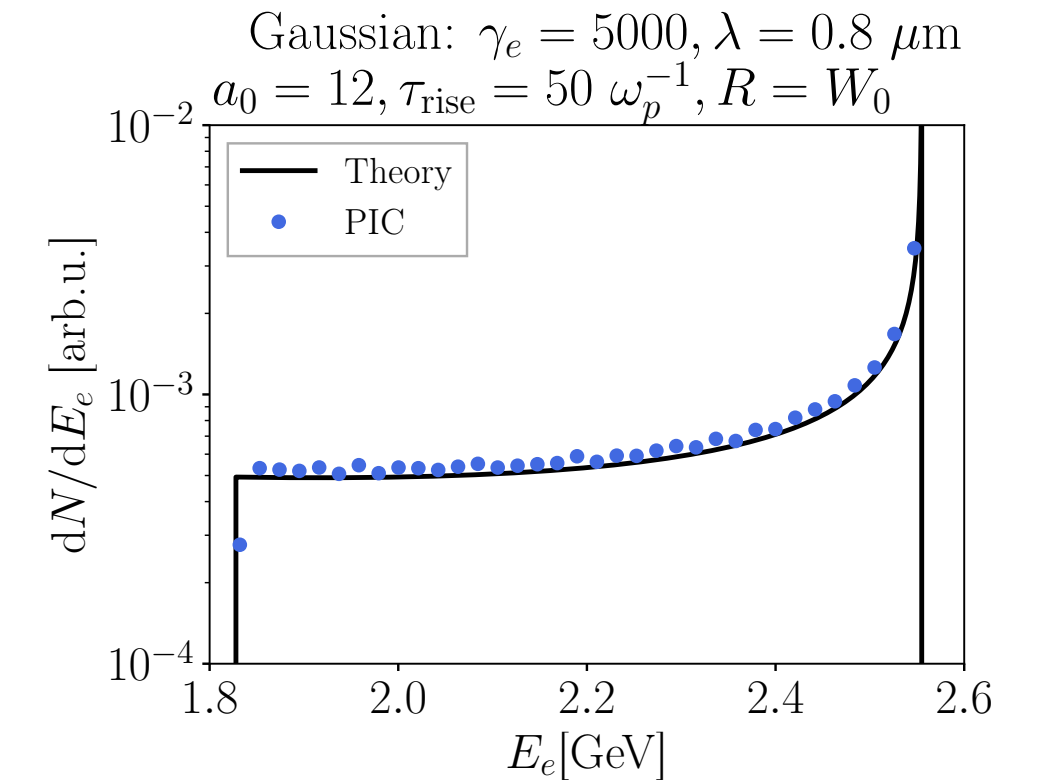
Spectra in focused scattering

Short beam $L \ll z_R$



In Classical Radiation Reaction regime we can exactly predict the final spectrum.

We can reconstruct the final e^- spectrum in focused scattering (Gaussian laser) by linear combination of Plane-Wave datasets.

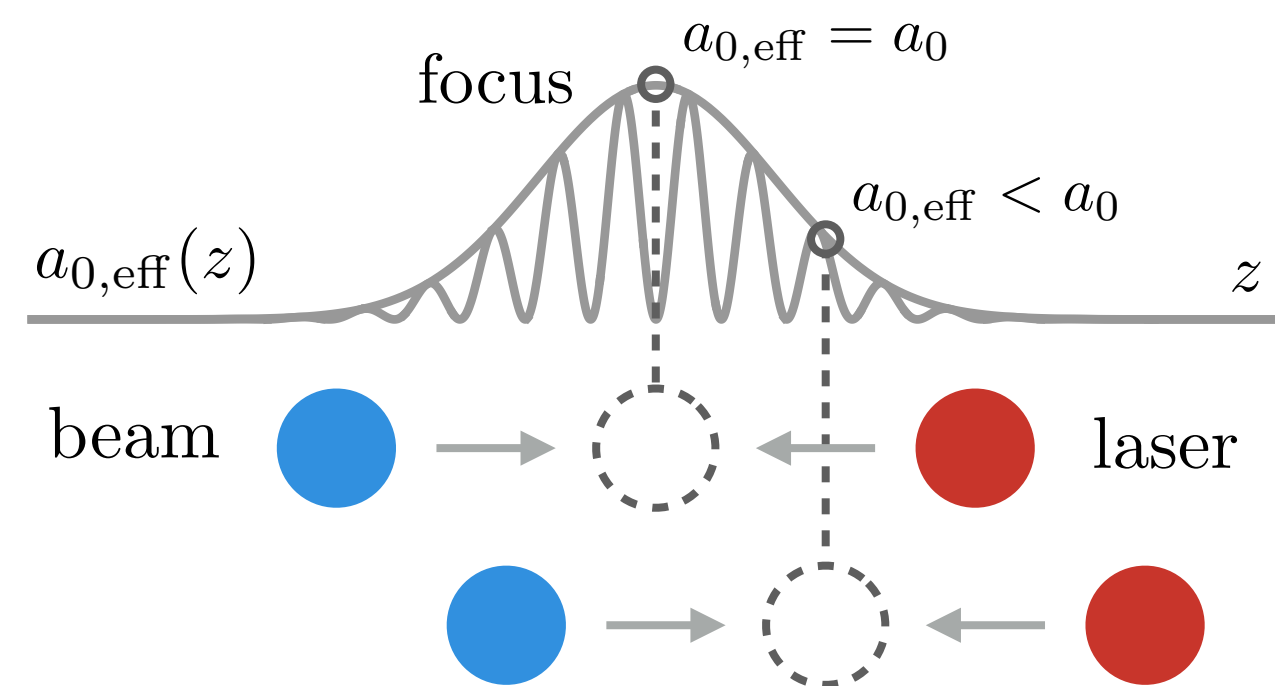


Particle distribution in laser field

In focused lasers * :

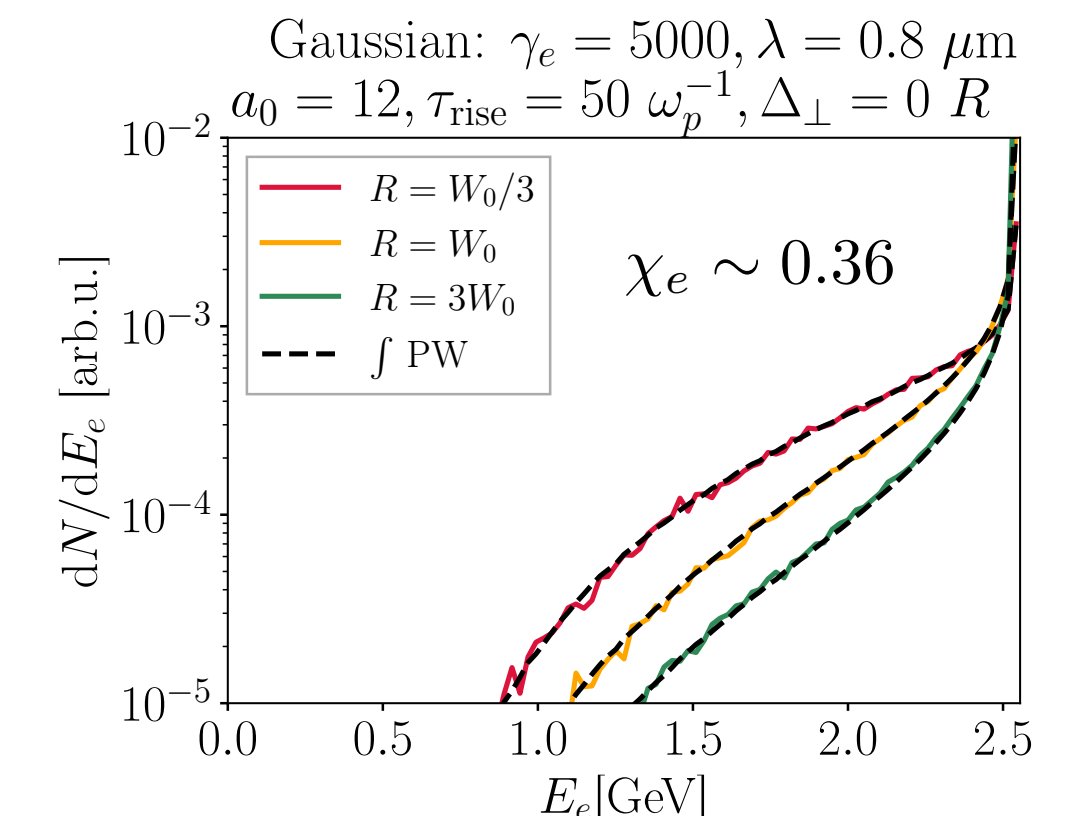
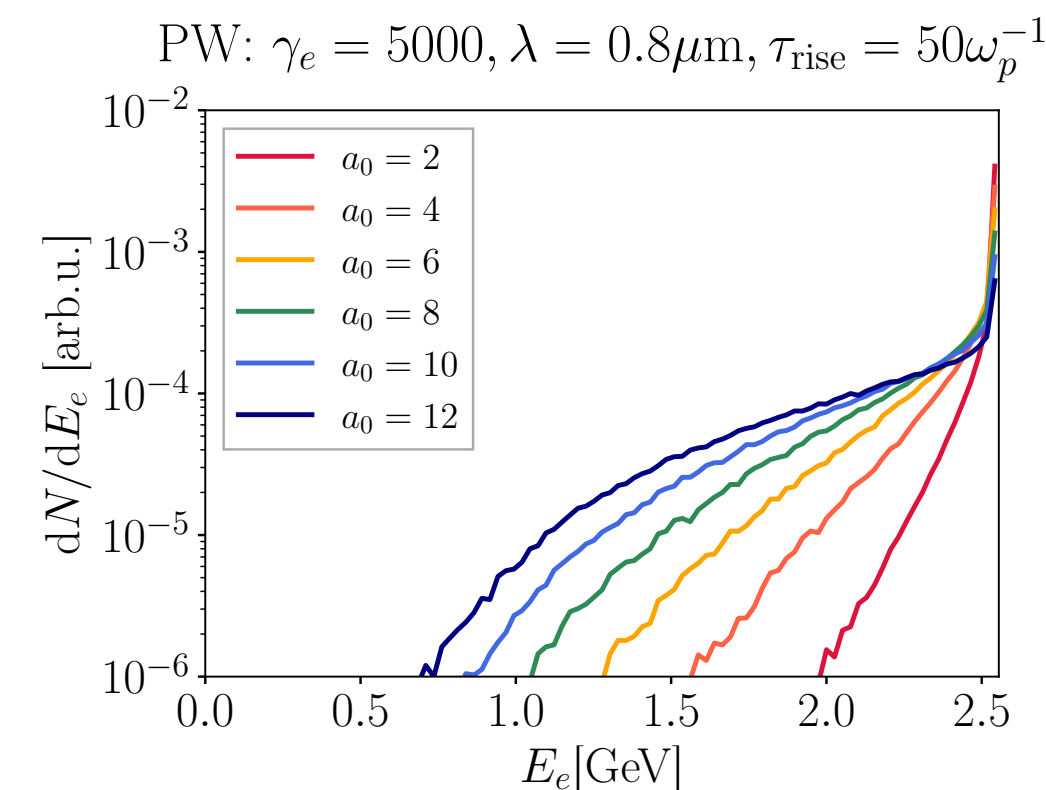
particles interact with different laser peak fields

We can apply $a_{0,eff}$ distributions to generalize models beyond the Plane Wave.



* Óscar Amaro and Marija Vranic 2021 New J. Phys. **23** 115001

$$\frac{dN_e^G}{d\gamma_e}(\gamma_e, a_0) = \int_0^{a_0} \frac{dN_e^{PW}}{d\gamma_e}(\gamma_e, a_{0,eff}) \frac{dN_b}{da_{0,eff}}(a_{0,eff}) da_{0,eff}$$



Synchrotron cooling as a progenitor of kinetic instabilities and coherent radiation.

Pablo J. Bilbao & Luis O. Silva

Synchrotron cooling in B_0 fields analytical model

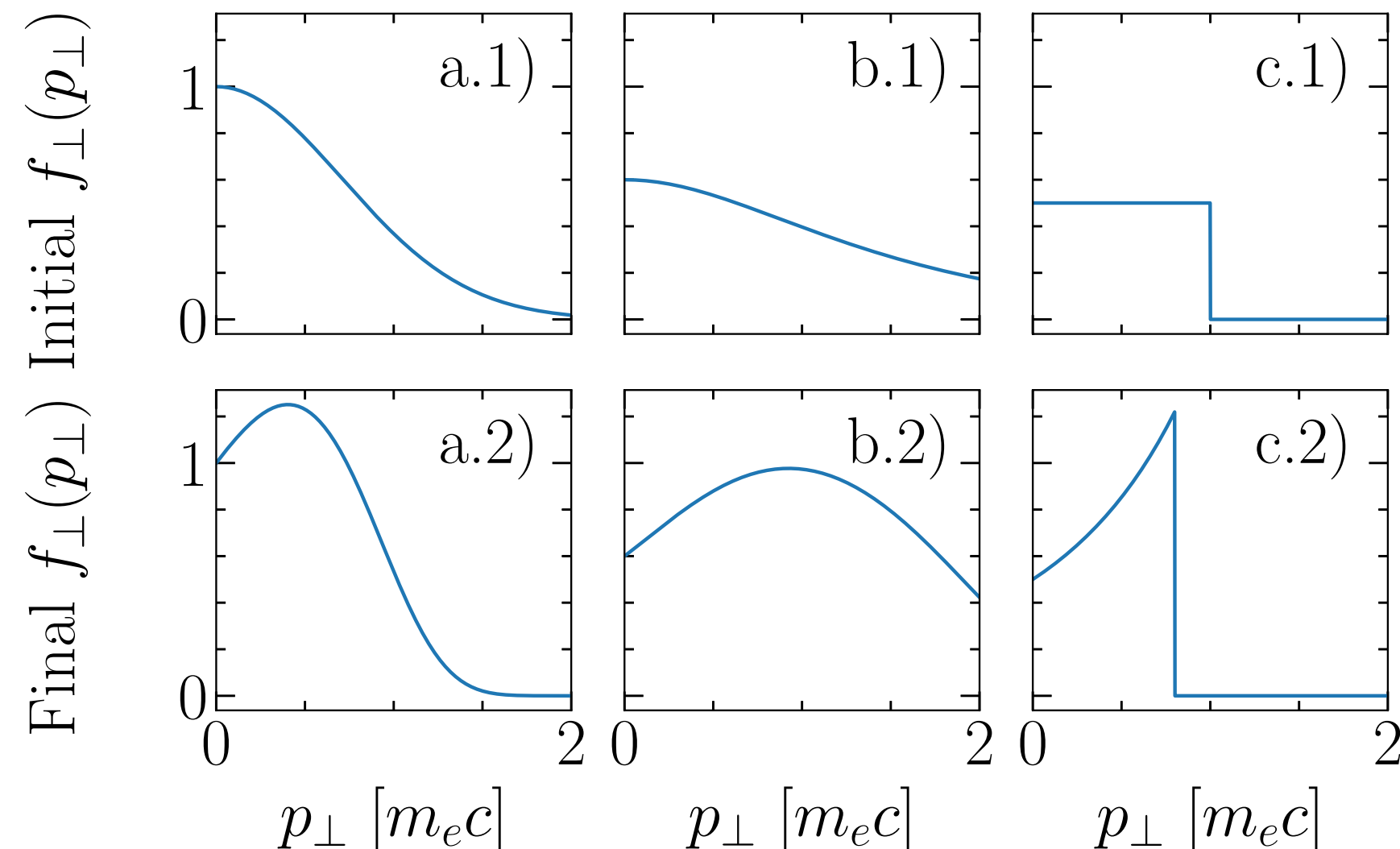
Particles undergoing Synchrotron cooling cool down at different rates

$$\dot{\mathbf{p}}_{RR} = -kB_0^2 \frac{p_{\perp}^2}{\gamma} \mathbf{p}_{RR}$$

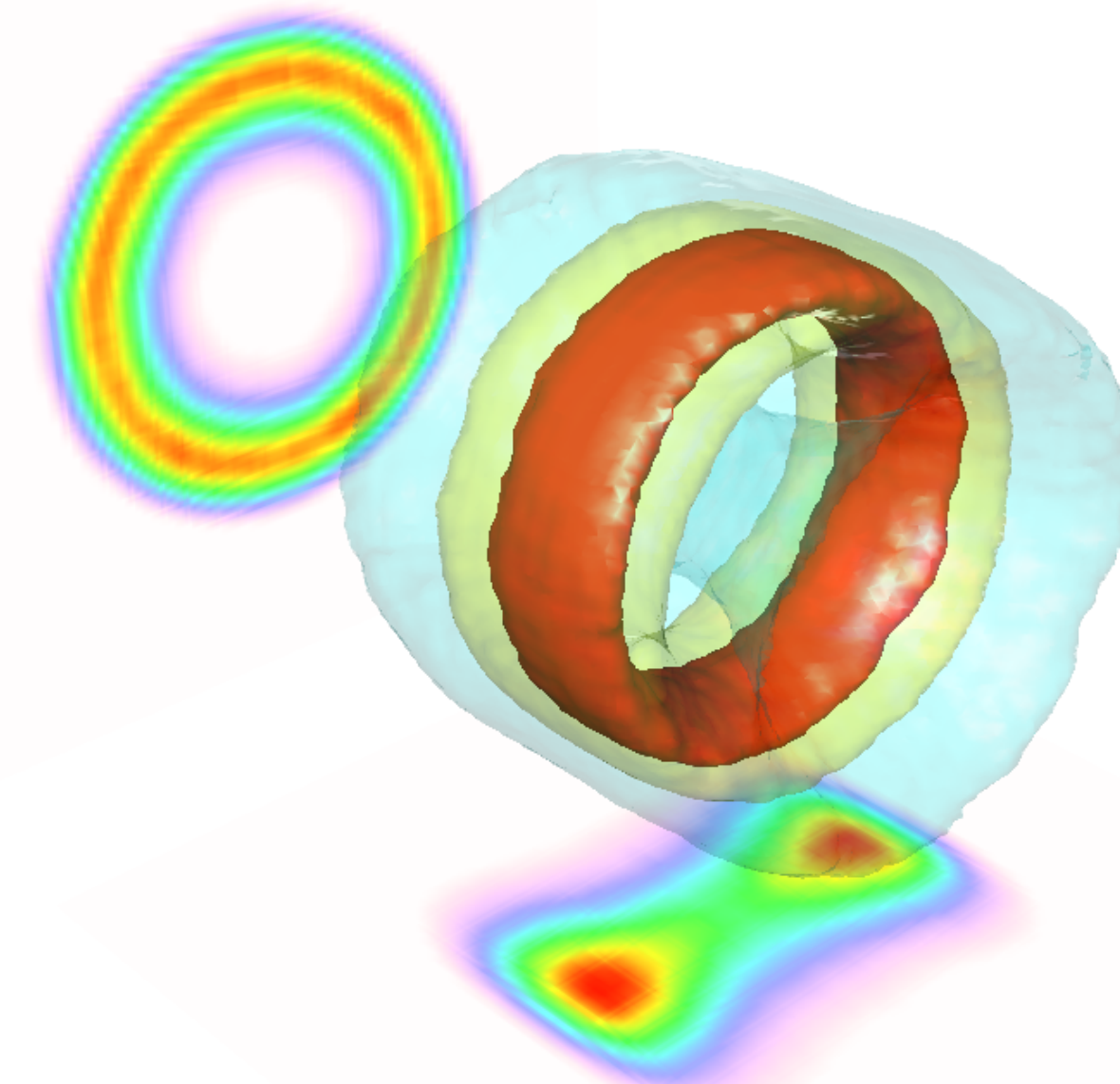
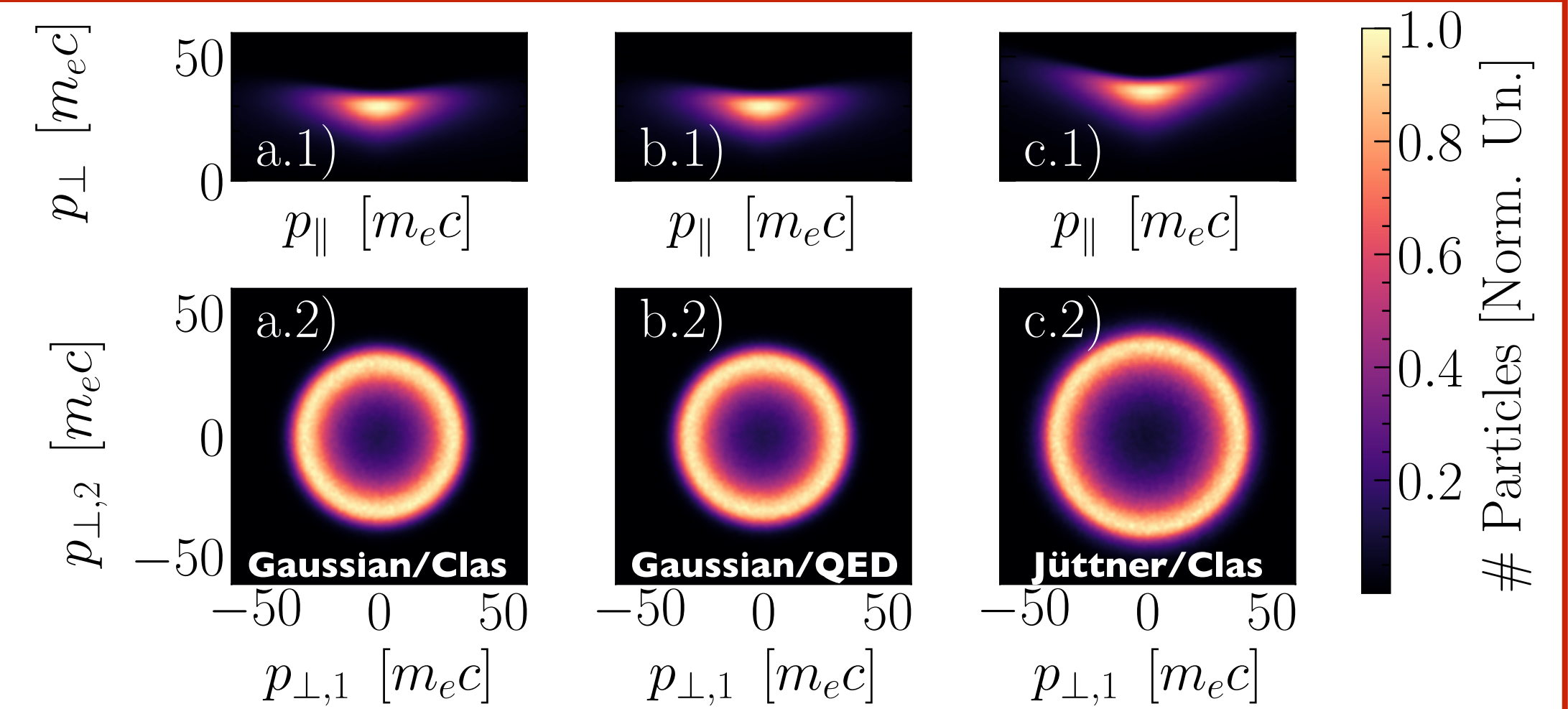
How does this affect collective plasma dynamics?

$$\frac{\partial f}{\partial t} + \dot{\mathbf{p}}_{RR} \cdot \nabla_p f + f \nabla_p \cdot \dot{\mathbf{p}}_{RR} = 0$$

So we demonstrate analytically that a Landau population inversion takes place for any arbitrary momentum distribution



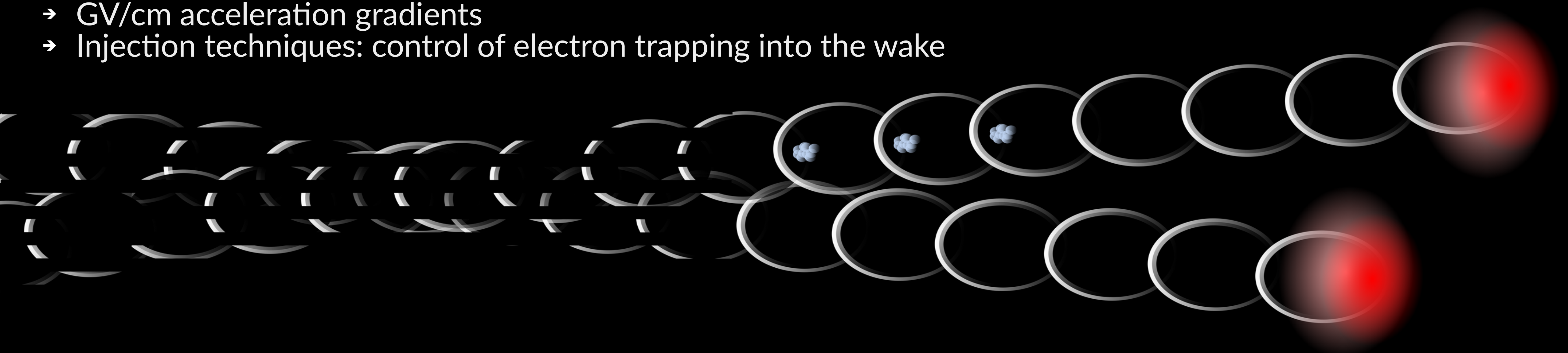
Simulations confirm our analytical results



Transient Relativistic Plasma Grating to Tailor High-Power Laser Fields, Wakefield Plasma Waves, and Electron Injection

Laser wakefield acceleration

- Plasma wakefield wave driven by an ultrashort laser pulse
- GV/cm acceleration gradients
- Injection techniques: control of electron trapping into the wake



New optical injection method

- Collision of two laser pulses at 10°
- Transverse plasma electron grating responsible for the injection
- Role switching of the driver and injector pulses
- Mutual injection into both wakefields
- Acceleration in later periods



HEDLA 2022

Flash Poster Presentation

<p>#03 D. Russell <i>Radiatively cooled shocks in jets at the MAGPIE pulsed-power facility</i></p>	<p>#04 K. Sakai <i>Local measurements of laser-driven electron-scale magnetic reconnection</i></p>	<p>#08 V. Tranchant <i>New Class of Laboratory Astrophysics Experiments: Application to Radiative Accretion Processes Around Neutron Stars</i></p>	<p>#09 F. Cruz <i>Particle-in-cell simulations of laser-driven, ion-scale magnetospheres in laboratory plasmas</i></p>	<p>#10 H. Hasson <i>Experimental results from a pulsed-power platform to study accretion-driven astrophysical outflows</i></p>
<p>#12 E. Figueiredo <i>Kinetic models in neutron star charge starved vacuum gaps</i></p>	<p>#13 S. Antunes <i>Time resolved opacity maps of warm dense Ti: a Bayesian search of coupling parameters</i></p>	<p>#18 R. Babjak <i>Direct laser acceleration enhancement using plasma density modulations</i></p>	<p>#19 B. Martinez <i>Ultra-high-intensity lasers for channel acceleration of positrons</i></p>	<p>#21 W. Zhang <i>Strong-field QED features in the leptonic beam collision</i></p>
	<p>#22 O. Amaro <i>Electron beam and photon distribution functions after a laser-electron scattering: analytical model accounting for 3D focusing geometry and non-ideal spatio-temporal synchronization</i></p>	<p>#25 P. Bilbao <i>Synchrotron cooling as a progenitor of kinetic instabilities and coherent radiation</i></p>	<p>#31 D. Maslarova <i>Transient Relativistic Plasma Grating to Tailor High-Power Laser Fields, Wakefield Plasma Waves, and Electron Injection</i></p>	